

Rainfall analysis in the contest of climate change for Jeddah area, Western Saudi Arabia

Ali M. Subyani¹ · Amjad F. Hajjar²

Received: 26 December 2014 / Accepted: 10 September 2015 / Published online: 24 February 2016
© The Author(s) 2016. This article is published with open access at Springerlink.com

Abstract The increase in the greenhouse gas emission has had a severe impact on global climate change and is bound to affect the weather patterns worldwide. This climate change impacts are among the future significant effects on any society. Rainfall levels are drastically increasing with flash floods in some places and long periods of droughts in others, especially in arid regions. These extreme events are causes of interactions concerning environmental, socio-economic, and cultural life and their implementation. This paper presents the detailed features of dry and wet spell durations and rainfall intensity series available (1971–2012) on daily basis for the Jeddah area, Western Saudi Arabia. It also presents significant articles for combating the climate change impacts on this area. Results show trend changes in dry and wet spell durations and rainfall amount on daily, monthly, and annual time series. Three rain seasons were proposed in this investigation: high rain, low rain, and dry seasons. It shows that the overall average dry spell durations is about 80 continuous days while the average wet spell durations is 1.39 days with an average rainfall intensity of 8.2 mm/day. Annual and seasonal autorun analyses confirm that the rainy seasons are tending to have more intense rainfall while the seasons are becoming drier.

This study would help decision makers in future for water resources management and flood risk analysis.

Keywords Climate change · Dry and wet spell · Daily rainfall · Jeddah · Saudi Arabia

Introduction

In arid regions environments, knowledge of the spatial and temporal variability, shifts, and trends of rainfall are important for water resources and planning under the global warming effects. This variability causes an impact on human life and cultural activities. The climate change causes an average temperature increase in the troposphere (Crutzen and Zimmermann 1991). Even 1 °C increase in the global temperature leads to about 250 to 300 km climate belt shifts from the equator towards the Polar Regions (Şen 2009). According to the IPCC (2007) report, until the end of the twenty-first century, the global temperature increase is expected to reach about 3.5 to 5 °C, which implies additional increases in the frequency and amount of different weather events leading to extraordinary hydrological phenomena as floods, droughts, water shortages, or stresses as well as on the agricultural productivity (Artlert et al. 2013).

Several studies were carried out on the analysis of rainfall variability and distribution in time as well as in space throughout the world. For instance, Akinremi et al. (2001) reported that there has been a significant increase in rainfall events by 29 % in Canadian prairies. Şen (2009) presented a methodology to predict future monthly rainfall amounts and surface runoff volumes on decadal basis from 2000 to 2050 in Istanbul (Turkey) and, accordingly, presented interpretation of monthly dry and wet periods. Goyal (2014) analyzed the precipitation variation and trend in Assam (India) from 1901 to

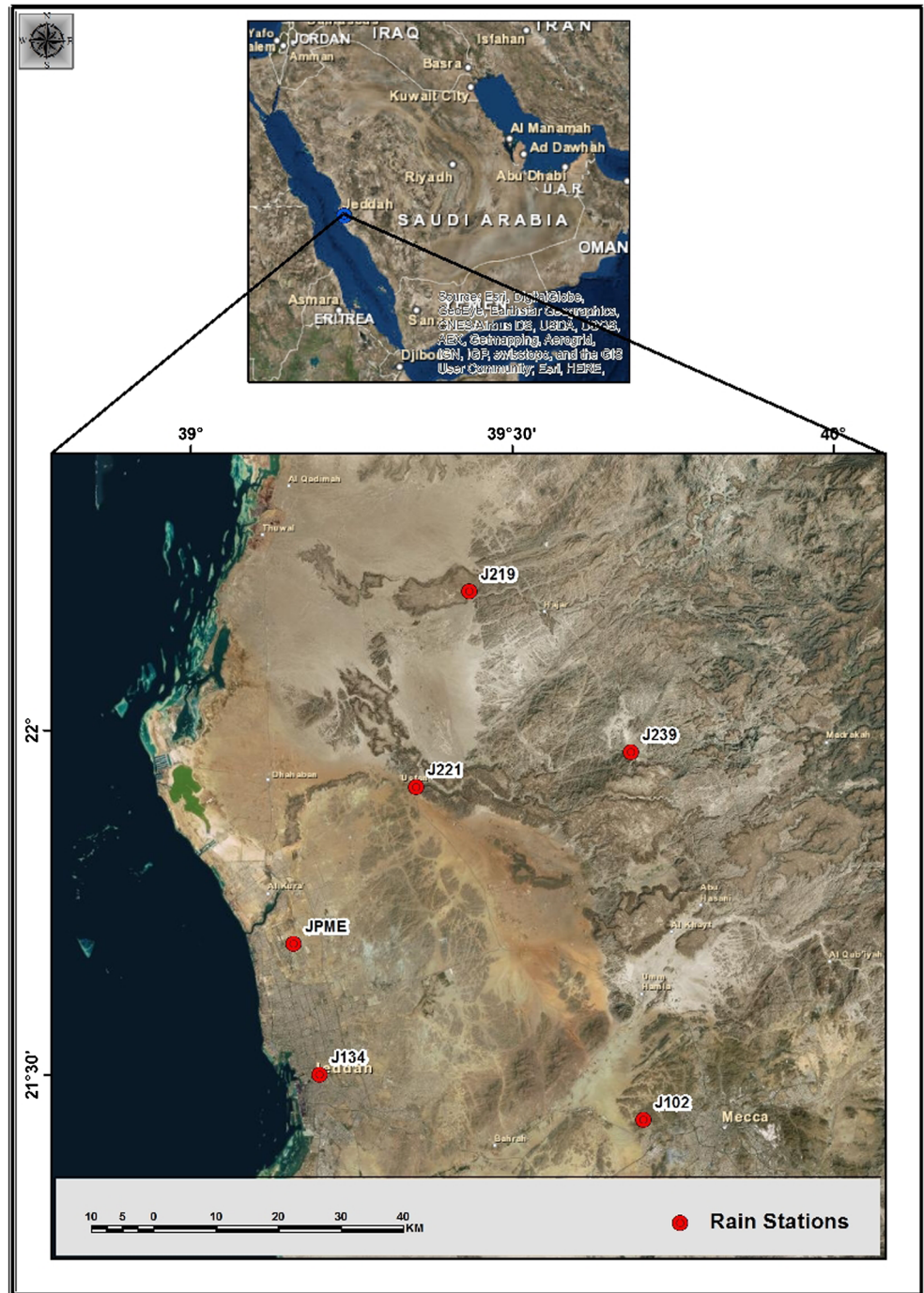
✉ Ali M. Subyani
asubyani@hotmail.com

Amjad F. Hajjar
ahajjar@kau.edu.sa

¹ Department of Hydrogeology, Faculty of Earth Sciences, King Abdulaziz University, P.O. Box 80206, Jeddah 21589, Saudi Arabia

² Department of Electrical and Computer Engineering, King Abdulaziz University, P.O. Box 80204, Jeddah 21589, Saudi Arabia

Fig. 1 Location map of the study area



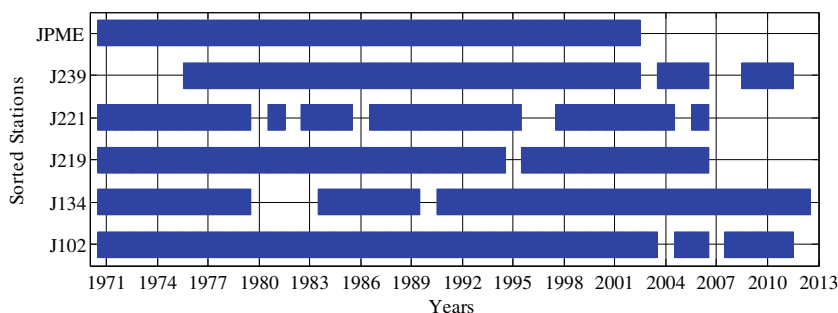
2002 in both annual and seasonal records. From time series analysis, he concludes that near normal occurrences happen in about 68 years out of 102 years, and if 2.48 years out of 102 years, there was an extremely wet period.

In Saudi Arabia, rainfall can be described as being little and irregular yet very extensive during the local storms. The western part of Saudi Arabia receives a moderate amount of rainfall with long memory of dry periods due to its geographic nature and location within the subtropical zone (Şen 1983; Alyamani and Şen 1992; Subyani 2004, 2011; Almazroui

Table 1 Distances between rainfall stations (km)

	J134	J219	J221	J239	JPME
J102	52	90	66	55	62
J134		83	48	69	24
J219			32	35	60
J221				35	27
J239					58

Fig. 2 Jeddah rainfall stations coverage (1971–2012)



2011). Knowledge and prediction of wet and dry spell probability occurrence, rainfall variability, shifts, and trends are critical when considering the impact of the climate change and can be estimated with reliability from reasonably available records. Wet and dry sequences are treated by different authors (Feyerhem and Bark 1965; Lioubimtseva 2004; Şen 2009; Almazroui et al. 2012).

The main objective of the present study is to identify the characteristic temporal and spatial variations of the rainfall on daily, monthly, and annual bases using classical statistical methods and properties of the wet and dry durations by fitting the best suitable probability density functions. Seasonal spells are also presented in this study. The proposed methodology are applied to the observed daily rainfall records for 1971–2012 from six rainfall stations located in Jeddah area, Kingdom of Saudi Arabia (KSA).

Study location and rainfall data

Jeddah area, located in the middle part of the Red Sea of Western Saudi Arabia (Fig. 1), is classified under the hot

weather conditions on the average. In addition to the extraordinary increase in frequency, occurrence and amount of extreme events (floods and droughts) are observable in many parts of the world. It is important to anticipate what similar cases might happen in the future climate around Jeddah area. Jeddah area has received unexpected amounts of rainstorms of 80 and 124 mm/day in 25 November 2009 and 26 January 2011, respectively. Today, there are 3.4 million people living in Jeddah with an annual growth rate of 3.5 % in an area of about 5460 km². The analysis of temporal and spatial wet and dry spell durations and rainfall intensity on the daily basis is necessary for an effective future urban planning and management for the city.

There are six meteorological stations in Jeddah area (J102, J134, J219, J221, J239, and JPME), where the daily rainfall records are available as shown in Fig. 1 (Ministry of Water and Electricity, Hydrology Division 2012). The period from 1971 to 2012 is selected over the entire study area. Table 1 illustrates the distances among the stations. Unfortunately, there are times where some of the stations are out of service. Considering the period from 1 January 1971 until 31 December 2012, the missing data points are on the average 18 % across all the stations. Figure 2 shows the coverage of each station from 1971 until the end of 2012. At any single period of time, one or more stations are active, which gives the opportunity to fill the gaps through spatial interpolation methods with the minimum root mean square error (RMSE) using the inverse distance method (Davis 2002). For a missing data point of a

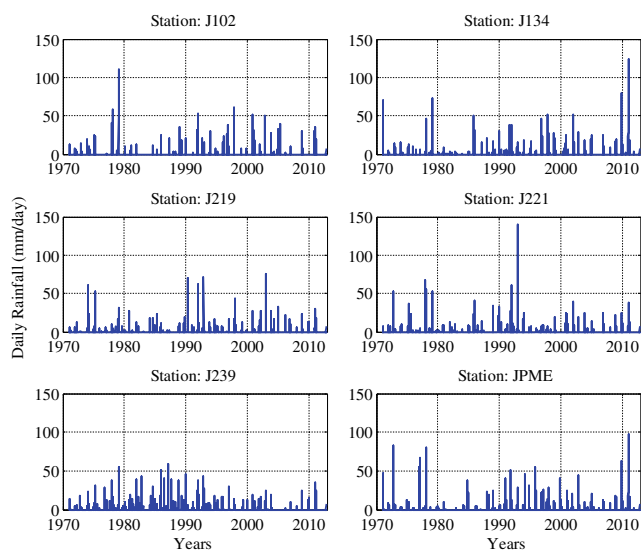
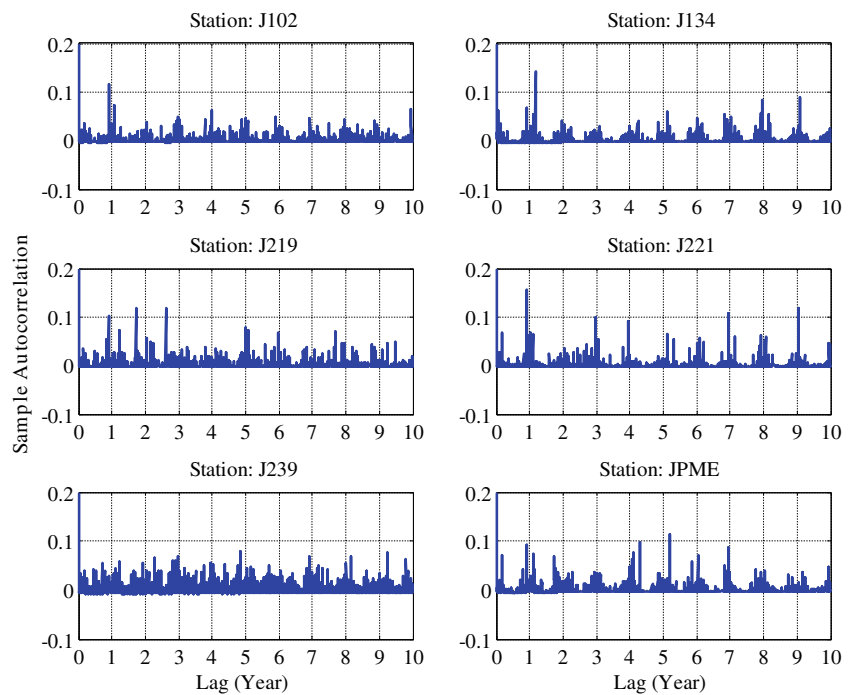


Fig. 3 Daily rainfall of Jeddah stations (1971–2012)

Table 2 Daily rainfall statistics and correlation coefficients between stations

	μ	σ	J134	J219	J221	J239	JPME
J102	0.121	2.020	35 %	18 %	25 %	18 %	0 %
J134	0.133	2.124	–	14 %	20 %	15 %	8 %
J219	0.108	1.712		–	28 %	23 %	4 %
J221	0.121	1.976			–	30 %	1 %
J239	0.157	1.834				–	0 %
JPME	0.149	2.214					–

Fig. 4 Autocorrelation functions of daily rainfall



given station, the filled value is the weighted average of the available stations nearby as follows:

$$y = \frac{1}{W} \cdot \sum_{i=1}^n \frac{x_i}{d_i^2} \tag{1}$$

where x^i is the rainfall at station i on the missing day, and d^i is the distance between the station of missing data point and station i , and hence, the weights are expressed by the following expression:

$$W = \sum_{i=1}^n \frac{1}{d_i^2} \tag{2}$$

Rainfall characteristics

Rainfall occurrences in Jeddah area can be described as very scarce and irregular, but very extensive during local storms. The rate of evaporation is very high. In addition, rainfall variability is extremely high and violent as is normally in the case of arid regions (Şen 1983; Subyani 2012). This area receives a moderate amount of rainfall compared with the rest of the country, due to the moderate elevations and the location within the subtropical zone. In addition, rainfall occurs in sporadic spatial and temporal nature in the study area, where the climate is affected by warm and moist tropical air mass from the tropical belt and Arabian Sea and cold polar air mass. In the following sections, the rainfall data is presented and analyzed

Fig. 5 Cross-correlation between significant correlated stations (see Table 2)

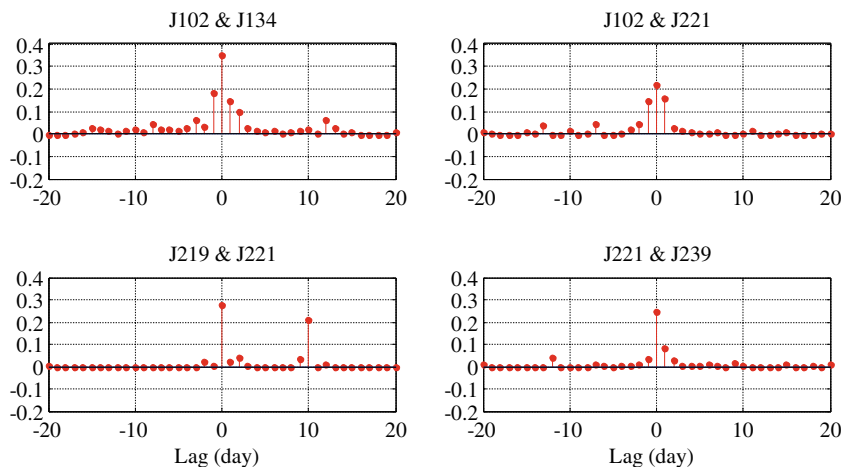


Table 3 Maximum daily rainfall occurrences since 1971

Station	J102	J134	J219	J221	J239	JPME
Date	16 Jan 1979	26 Jan 2011	11 Jan 2003	13 Dec 1992	8 Mar 1987	2 Nov 1972
Rainfall (mm)	110.5	124.0	75.2	140.2	58.6	83.0

from different angles for better understanding the rainfall characteristics in this arid region.

Daily rainfall

First, the daily rainfall data time series of the six stations are presented in Fig. 3, which shows the high variations in rainfall amounts throughout the 42 years as the normal situation in arid regions. The basic statistics of this data are given in Table 2. On the average across all stations, the daily rainfall mean value is 0.13 mm/day with a standard deviation of 1.98 mm/day. This general statistics may not be informative; a better statistics would be to separate the rainy days data from the dry ones. The probability of a rainy day at the different stations ranges from 0.86 to 2.9 % (1.8 % on the average). Given that it is raining in a day, the expected rainfall is 8.32 mm/day.

In studying the rainfall correlation coefficient between the different stations, it is found that the highest value is 35 % between stations J102 and J134. Although the distance between these two stations is not the minimum, but they are located in the same synoptic situation and associated cloud stream. The airport station (JPME), on the other hand, has almost no correlation to any other station even though it is very close to station J134. It shows that the rain in this region is highly variable spatially and unpredictable on the daily bases.

A better statistics of rain variability is the sample autocorrelation function (ACF) defined as (Box et al. 1994):

$$ACF(k) = \frac{\sum_{i=1}^{N-k} (x_i - \mu_x) \cdot (x_{i+k} - \mu_x)}{\sum_{i=1}^N (x_i - \mu_x)^2} \tag{3}$$

where x_i for $i=1$ to N is the data samples, μ_x is the sample mean value, and k is the lag index in days. In case of missing

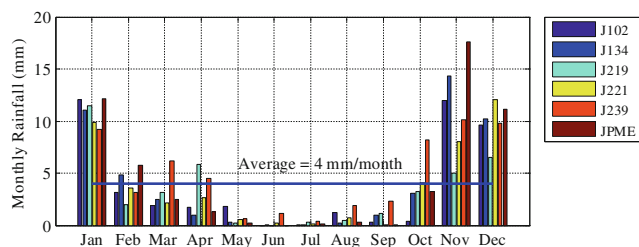


Fig. 6 Average monthly rainfall

data point, one might standardize the samples and then replace the missing data points by zeroes as suggested by Cryer (1986). The ACF for the daily rainfall of each station is calculated for 3650 days of lag, i.e., 10 years lag (Fig. 4). As can be seen from the figure, weak annual repeatability is presented, but no significant values exist (below 0.2).

In regard to the cross-correlation between the stations at different lag days, Fig. 5 shows the significant records only. Note that the correlations at lag zero are linear correlation coefficients. The figure says that when it rains in one station, there is a chance that it would rain in the next day (or the day before) on the other station. The significant correlation coefficients occur at lags ± 1 day at the most.

Interestingly, however, if it rains at station J219, then there is a 28 % chance that it will also rain at station J221 in the same day, and a 20 % chance in the next 10 days. Mind the reader that this statistics is based on the records of 42 years, and this may be the result of the extension of the upper trough which deepens and causes widespread rainfall to the south.

Finally, for the daily presentation, the maximum reported rainfall of the stations and their corresponding dates are shown in Table 3. The flood reported lately on Jeddah in January 2011 coincides with the maximum reported rainfall of 124 mm/day at station J134 located at the heart of Jeddah City. Unlike the inurbane area around station J221, where 140.2 mm/day rainfall is recorded in 13 December 1992 without any reported incidents. The different dates of the maximum daily rainfall occurrences show that there is no consistency in the storm events in the study area.

Monthly rainfall

Next, the monthly rainfall is examined for the stations for better understanding of the rain behavior in different seasons. First, the average monthly rainfall for each month over the 42 years is shown for each station in Fig. 6. It is clear that the rainy months for most of the stations are November, December, and January with an overall average rainfall of 10.45 mm/month. In February, March, and April, the average

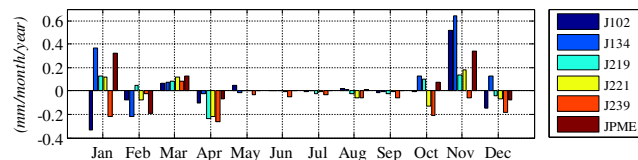
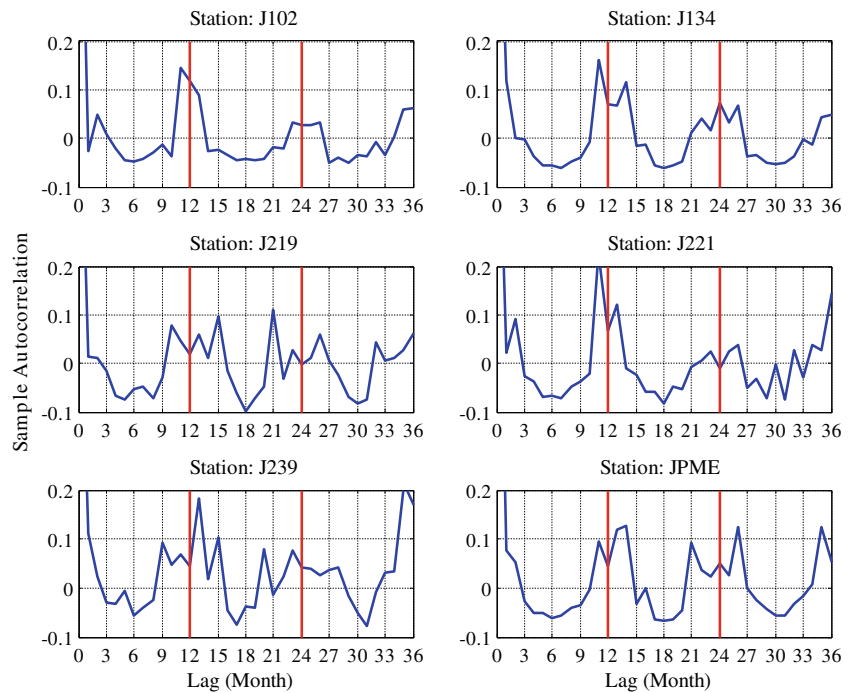


Fig. 7 Monthly rainfall trends

Fig. 8 Autocorrelation functions of monthly rainfall



is 3.27 mm/month, while in the remaining months the average rainfall is 1.02 mm/month. This might suggest classification of the rainy seasons for Jeddah area “month (average rainfall mm/month)” as follows:

- High rain season: November (11.2), December (9.9), and January (11.0)
- Low rain season: February (3.7), March (3.1), April (2.8), and October (3.7)

- Dry season: May (0.6), June (0.2), July (0.2), August (0.8), September (0.8)

A study of the rainfall linear trend is also presented for each month since 42 years ago. To assess the significance of the trends, the non-parametric Mann-Kendall test is utilized (Mann 1945; Kendall 1975). For the 12 different months and for the six different stations, Fig. 7 shows the linear trends of the monthly rainfall. With a significance of

Fig. 9 Trend behavior of annual rainfall

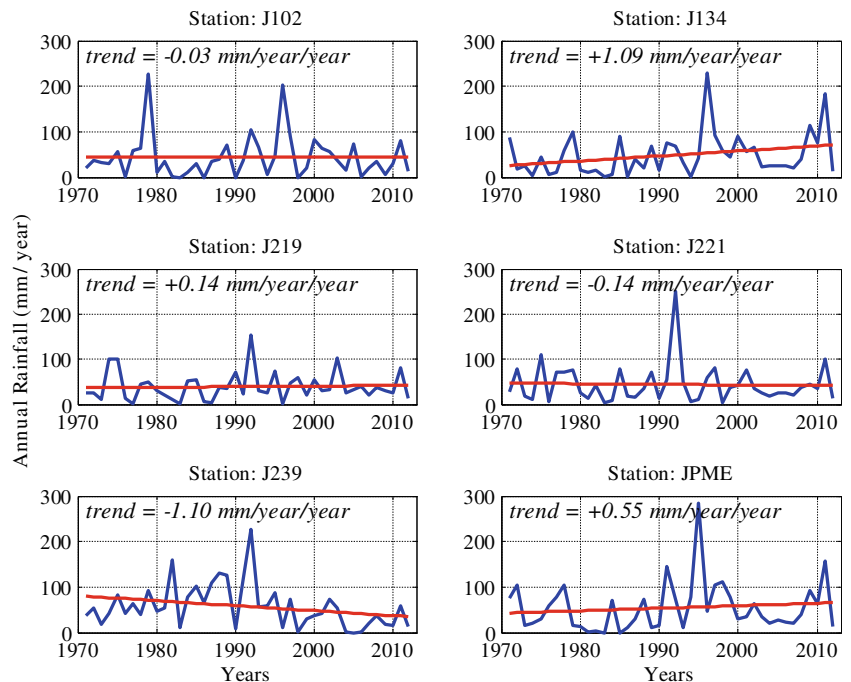


Fig. 10 Annual rainfall trend map

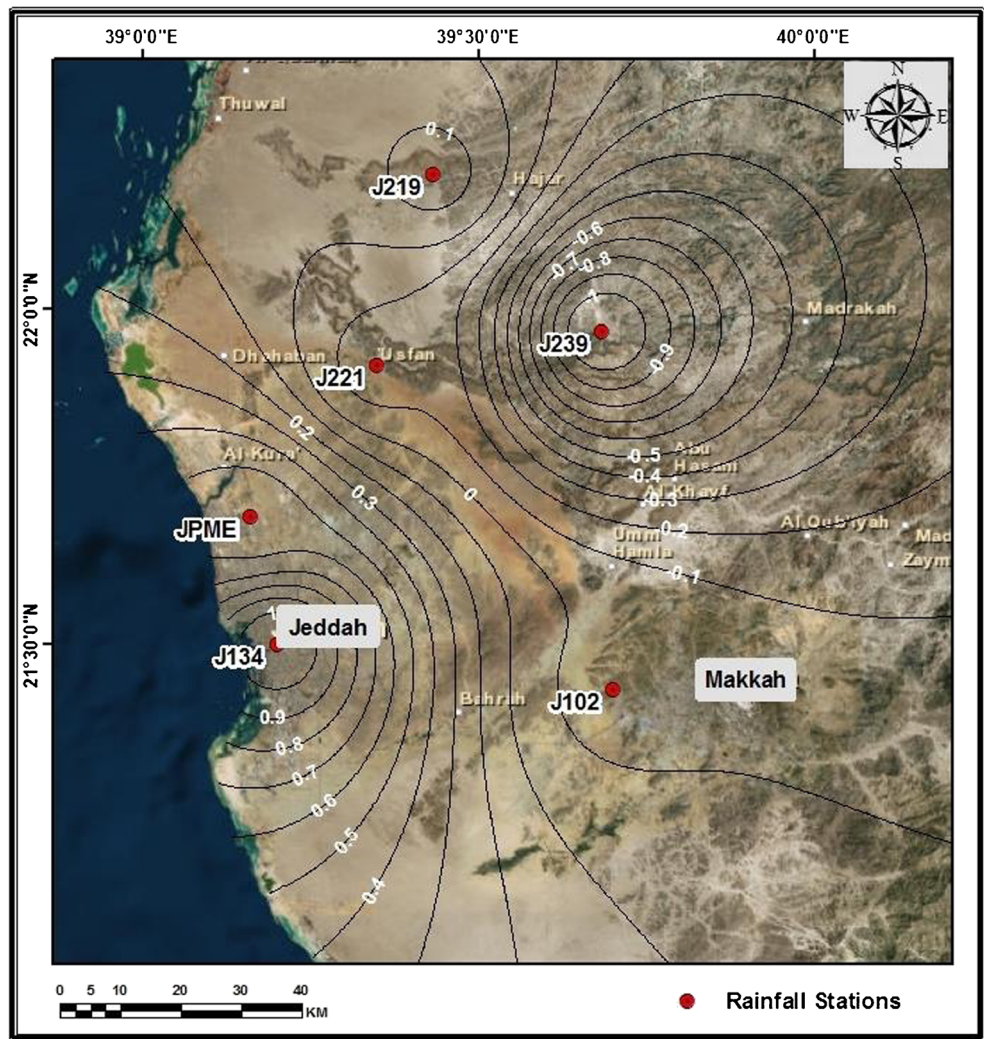
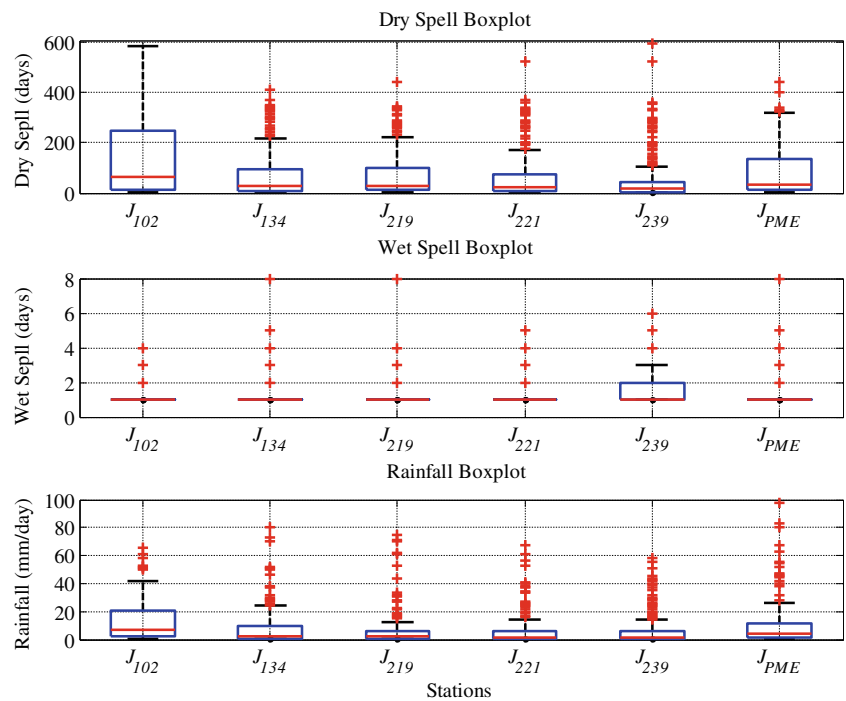


Table 4 Dry and wet spell duration and rainfall general statistics

		J102	J134	J219	J221	J239	JPME	averages
Dry spell (day)	Mean	134	79	73	64	46	84	80
	Std	159	111	94	94	80	104	107
	Median	62	27	28	25	16	32	32
	Q ₂₅ -Q ₇₅	14-246	8-93	10-97	7-73	5-46	13-136	10-115
	Max	703	644	439	523	593	439	557
Wet spell (day)	Mean	1.18	1.27	1.29	1.32	1.38	1.30	1.29
	Std	0.52	0.76	0.72	0.85	0.78	0.77	0.73
	Median	1.00	1.00	1.00	1.00	1.00	1.00	1.00
	Q ₂₅ -Q ₇₅	1-1	1-1	1-1	1-1	1-2	1-1	1-1
	Max	4.00	8.00	8.00	9.00	6.00	8.00	7.17
Rain (mm/day)	Mean	14.02	8.38	6.24	5.98	5.44	9.83	8.32
	Std	16.77	14.71	11.48	12.59	9.37	15.16	13.35
	Median	7.00	2.00	2.10	1.58	1.40	3.90	3.00
	Q ₂₅ -Q ₇₅	2.7-20.2	0.5-10	0.5-6.2	0.2-6.2	0.3-6.0	1.0-11.7	0.9-10.0
	Max	110.50	124.00	75.20	140.20	58.60	97.43	100.99

Fig. 11 Box plots for dry and wet spells and rainfall of the stations



95 %, station J134 has a linear positive trend of $+0.52$ mm/month per year in November, while station J239 has a negative trend of -0.22 mm/month per year trend in the month of January. If one considers the three seasons of rain as suggested above and average out the monthly linear trends across the stations, one can notice the following average linear trends:

- A positive trend in the high rain months of $+0.0977$ mm/month per year

- A negative trend in the low rain months of -0.0524 mm/month per year
- A negative trend in the dry months of -0.0099 mm/month per year

This yields a general conclusion that the rainy months tend to be more intense than before while the dry months are getting drier, which agrees with the global climate change trend (IPCC 2007). Further presentation shows a more interesting support to this conclusion.

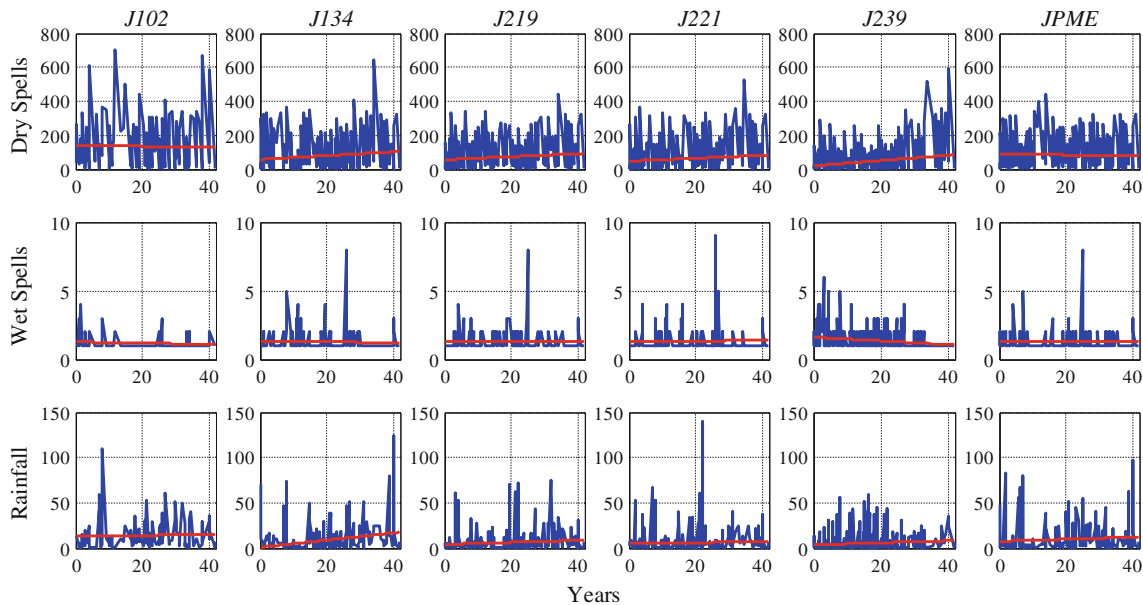


Fig. 12 Trends for daily dry and wet spells and rainfall intensities

Table 5 Trends for dry and wet spells and rainfall intensities with their MK tests

		J102	J134	J219	J221	J239	JPME	Average	
Dry spells	Trend	-0.181	+1.120	+0.880	+0.851	+1.572	-0.180	+0.68	(day/year)
	<i>p</i> value	0.67	0.02	0.18	0.50	0.29	0.94		
Wet spells	Trend	-0.004	-0.002	-0.001	+0.004	-0.014	-0.002	-0.00	(day/year)
	<i>p</i> value	0.97	0.56	0.89	0.45	0.03	0.83		
Rainfall	Trend	+0.050	+0.400	+0.110	+0.060	+0.110	+0.110	+0.14	(mm/day/year)
	<i>p</i> value	0.23	0.00	0.01	0.04	0.00	0.00		

The autocorrelation function is also calculated based on the monthly rainfall data and results are shown in Fig. 8. Again no significant values were reported except for the annual behavior of the rain (12, 24, 36, and so on months). The autocorrelation values show irregularities due to the high variability of the rain.

Annual rainfall

The mean annual rainfall gives an idea about the general behavior of the rain in the area. The annual rainfall data for the six stations along with its linear trends fit for estimation is shown in Fig. 9. For some stations, the trend is positive while negative for the others. The computed *p* values of the Mann-Kendall tests are 0.71, 0.08, 0.42, 0.94, 0.06, and 0.39 for the stations J102, J134, J219, J221, J239, and JPME, respectively. The urban station J134 located at Jeddah City experiences a positive trend of 1.09 mm/year/year with a low *p* value (significance at 90 % confidence level) indicating a potential hazard for the city that must be taken into consideration in future planning. Station J239 located in the mountains outside the city indicates a significant but negative trend suggesting a shift or a decrease in rainfall occurrences along the coastal areas before reaching the mountainous regions in the east of Jeddah City. The rainfall increase is mainly due to the contribution of the southerly heat flux which creates instability and the moisture flux necessary for deep cloud formation. These two factors trigger cloud formation while orographic lifting increases the rainfall amount which explains the difference in rainfall amounts between the two areas. Figure 10 shows the annual

rainfall trends posted as a contour map to illustrate this behavior.

Autorun analysis

The classical statistics of the rainfall presented so far lacks the view of the rain sequential behavior with time. The studies by Şen (1976, 1978, 1985) investigated the statistical properties of the wet and dry durations of stream flow sequences in order to estimate the surplus and deficit magnitude within dry and wet periods. However, in this research, a mechanism for synthetic daily rainfall generation for Jeddah area needs to preserve the historical wet and dry spell properties. Such a generating model of synthetic sequences requires identification of a suitable parsimonious model. In addition to the classical statistical parameters such as mean, standard deviation, and serial correlation coefficients, the wet and dry period statistics are also considered as they are estimated from the available historical sequences.

Spell durations statistics

From the daily rainfall data for the different stations, the dry and wet spell durations are extracted as well as the rainfall intensity of the rainy days. Data are truncated at zero rainfall level in this study, since a little drop of rain is so precious in arid regions. The general statistics is shown in Table 4. As can

Table 6 Kolmogorov-Smirnov goodness of fit for dry spell durations

	J102	J134	J219	J221	J239	JPME	μ
Geometric	0.170	0.215	0.193	0.200	0.228	0.193	0.20
Logarithmic	0.245	0.222	0.240	0.205	0.185	0.265	0.23
D. Uniform	0.258	0.298	0.280	0.309	0.339	0.270	0.29
Poisson	0.618	0.678	0.665	0.670	0.678	0.647	0.66

Table 7 Kolmogorov-Smirnov goodness of fit for wet spell durations

	J102	J134	J219	J221	J239	JPME	μ
Poisson	0.670	0.637	0.632	0.620	0.597	0.628	0.63
D. Uniform	0.500	0.667	0.667	0.667	0.667	0.667	0.64
Geometric	0.707	0.687	0.683	0.676	0.663	0.681	0.68
Binomial	1.000	0.700	0.640	0.793	0.688	0.702	0.75
Logarithmic	0.856	0.800	0.793	0.776	0.746	0.788	0.79

Table 8 Kolmogorov-Smirnov goodness of fit for rainfall intensities

	J102	J134	J219	J221	J239	JPME	μ
Log-Pearson 3	0.051	0.037	0.083	0.079	0.121	0.046	0.070
Gen. Gamma (4P)	0.046	0.056	0.094	0.076	0.105	0.052	0.072
Weibull (3P)	0.047	0.059	0.125	0.055	0.098	0.047	0.072
Burr	0.050	0.060	0.086	0.078	0.111	0.055	0.073
Log-Logistic (3P)	0.060	0.066	0.078	0.073	0.116	0.052	0.074

be seen, the overall average dry spell duration is 80 continuous days, while the wet spell durations average is 1.29 days with an average rainfall intensity of 8.32 mm/day. From the maximum values for both wet and dry spells, one finds that it did not rain at all for 703 days (almost 2 years from May 1982 to August 1984) at the location of station J102, while at most it rained consecutively for 9 days at station J221 during November 1996. The median values give better statistics when extreme values occur in the data. It can be seen that the dry spell durations have medians between 16 and 62 days for the different stations, while the wet spells have median values of just 1 day across all stations. Finally, the 25 and 75 % percentiles of the data are reported, which show the values of the core data without outliers. On the average, across the six stations, the dry spell duration's 25–75 % percentiles ranges between 10 and 115 days, the wet spell durations are tightly ranged in 1 day, and the rainfall intensities range between 0.9 and 10 mm/day.

In regard to the distribution of the spells durations and rainfall intensity, their box plots are shown in Fig. 11. The

boxes extend between the 25th to the 75th percentiles (Q_{25} and Q_{75}) while the red marks indicate the data outliers outside the $Q_{75} + 1.5(Q_{75} - Q_{25})$ range. Notice for station J102 that the dry spells extend longer than the other stations, and in the meantime the rainfall intensities has many days of extreme rainfall with 100 mm/day at station JPME and 80 mm/day at station J134. With the wet spell durations being packed in the 1 day range, this indicates a potential flash flood occurrence of high risk in the urban areas.

When analyzing the dry and wet spell durations and the rainfall intensity over the years, the trends are observed at the different stations (Fig. 12). Each column of the figure represents the data of a station, whereas the rows show the dry spells, the wet spells, and the rainfall intensity, respectively. Table 5 lists the trends along with its Mann-Kendall p -values for testing them. On average, the dry spells have positive trends towards longer days. For the wet spells, there is no trend. For the rainfall intensities, there are positive significant trends for all stations confirming the potential threat of having intense rainfall in the future.

Spell duration distributions

The next step is to find the best probability mass function (or density function) for the dry and wet spell durations as well as the rainfall intensities of the rainy days. Besides, it is an essential step in the rainfall generation to find the best fitting distribution functions for the spell durations.

Fig. 13 CDF of dry spell for the stations

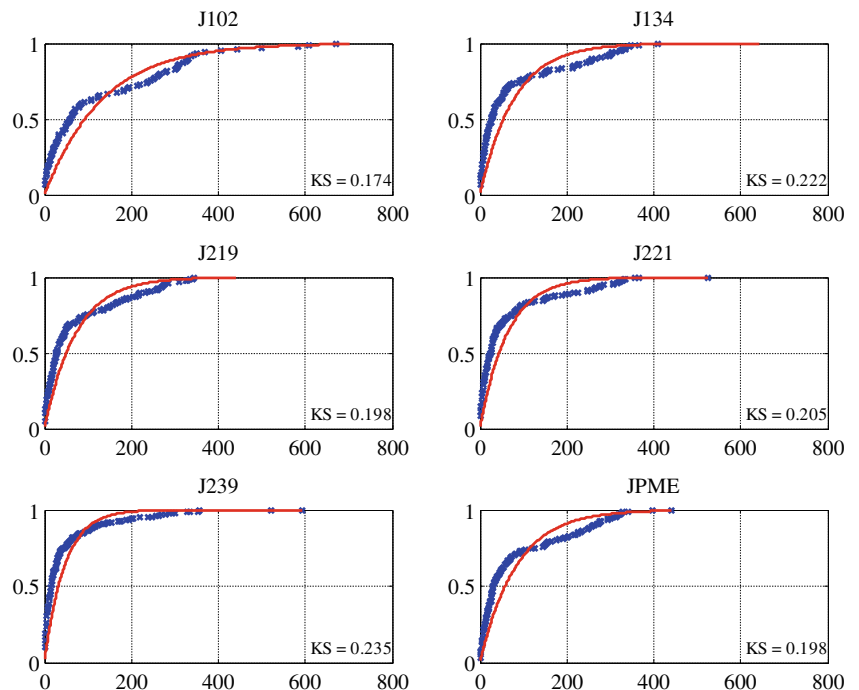
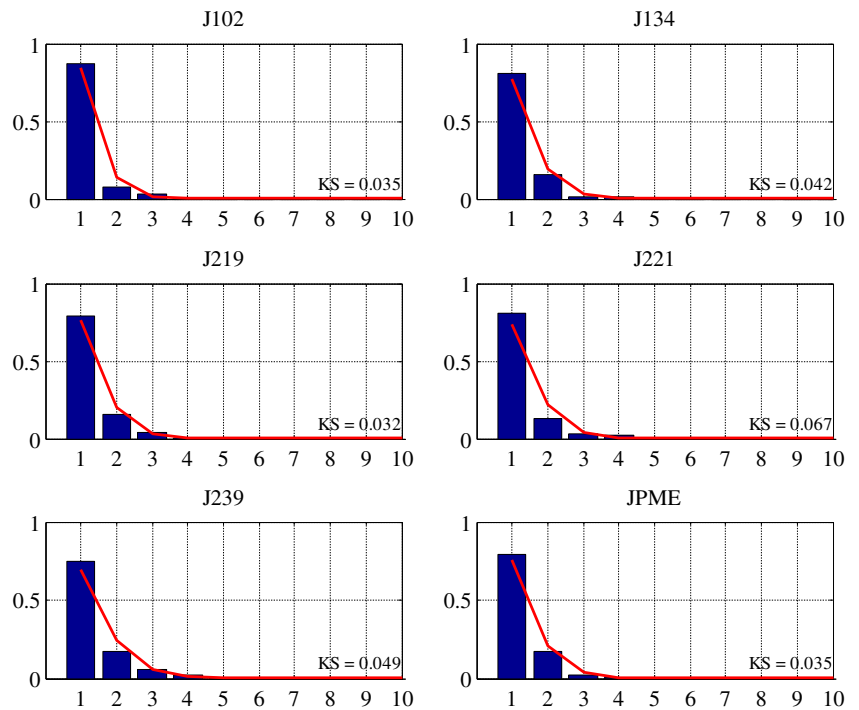


Fig. 14 PDF of wet spell for the stations



Utilizing the professional statistical software package (EasyFit software 2009), which includes numerous distribution functions, exhaustive fittings are performed on the data of the different stations. One can notice that the dry and wet spell durations are integer numbers with a minimum of 1 day, while the rainfall intensity is a continuous positive non-zero number.

Results of the best fittings adopting Kolmogorov-Smirnov (KS) goodness of fit are shown in Tables 6, 7, and 8 for the dry spells, wet spells, and the rainfall intensities, respectively. The last column in each table is added to show the average KS goodness of fit across all the stations in order to figure out the most suitable distribution function as follow.

Fig. 15 CDF of rainfall intensities for six stations

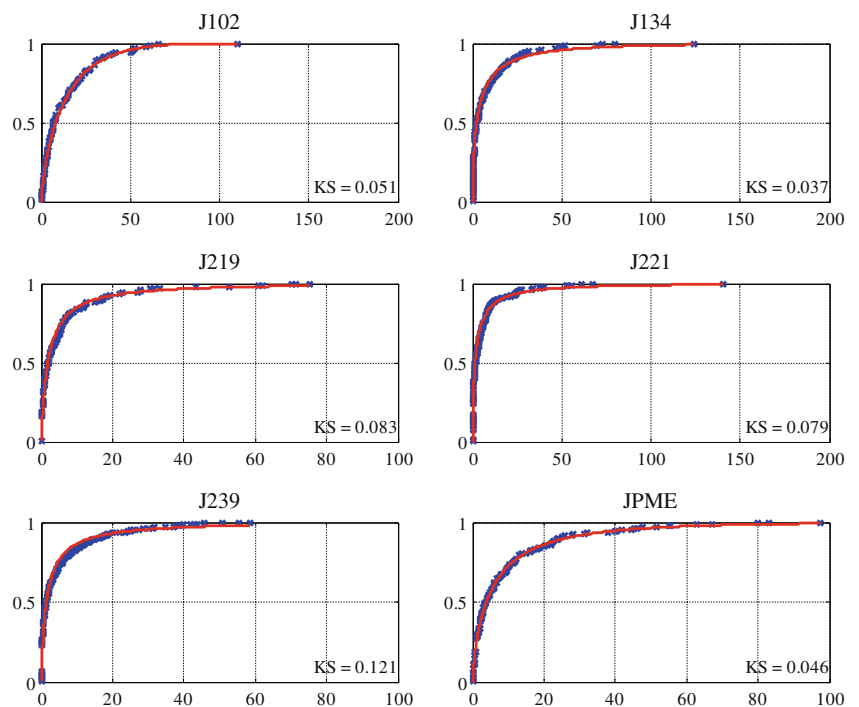


Fig. 16 Seasonal dry and wet spells and rainfall means

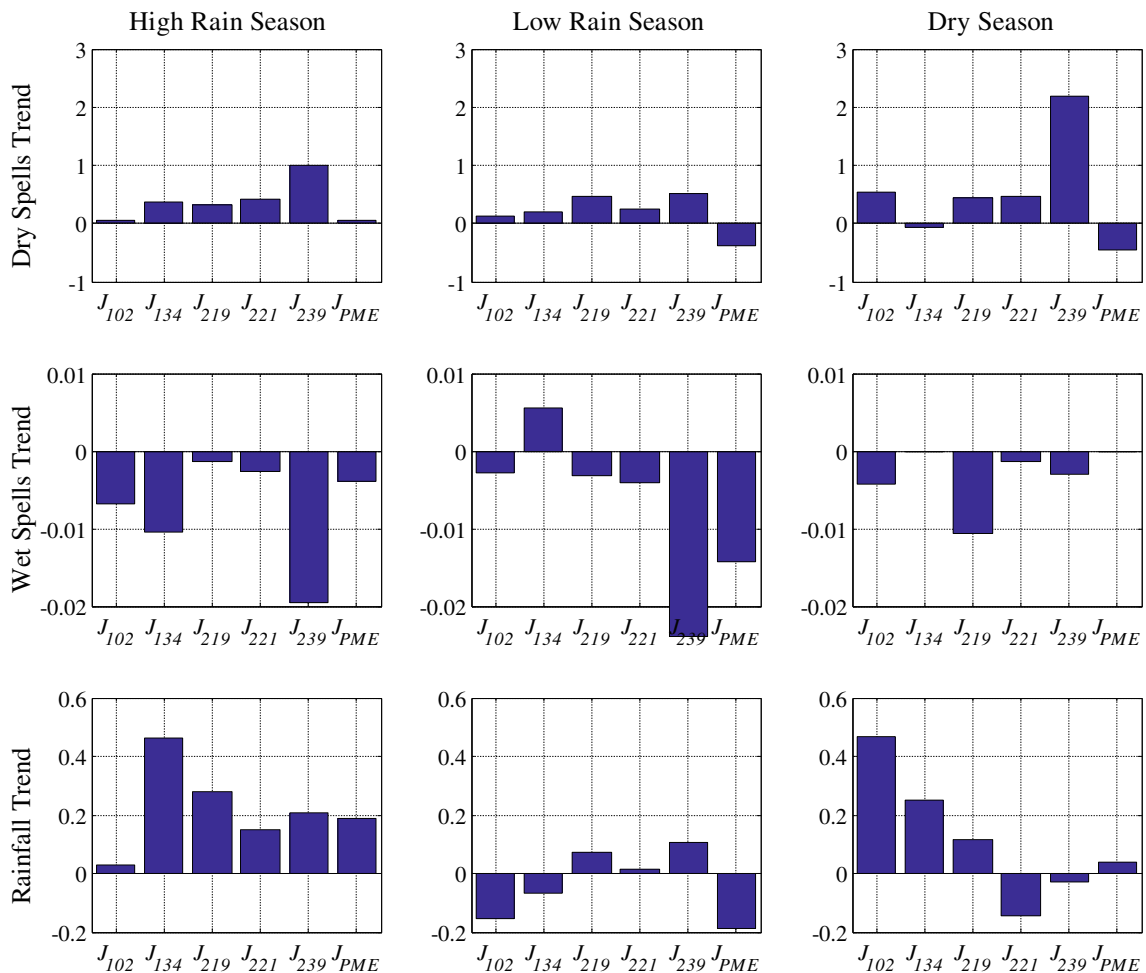
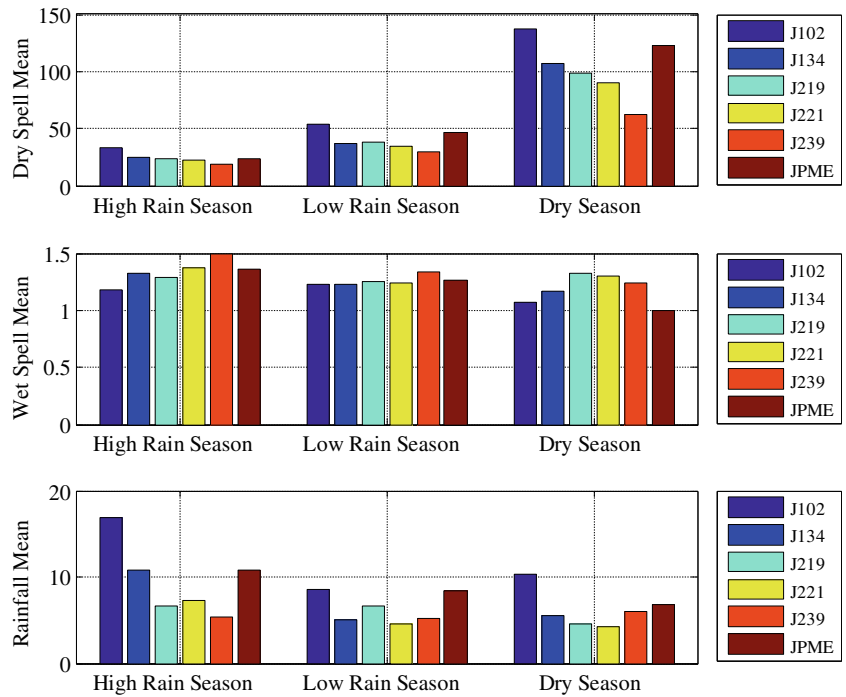


Fig. 17 Trends of seasonal dry and wet spells and rainfall intensities

- Dry spell durations are best distributed as Geometric
- Wet spell durations are best distributed as Poisson
- Rainfall intensities are best distributed as Log Pearson Type III

The fitted Geometric and Poisson functions for the dry and wet spell durations have discrete domains starting from zero to infinity; however, the spell durations are integer numbers with a minimum of 1 day, hence, one can adjust the distribution functions to have a discrete domain of $1 \leq x < \infty$ (Milton and Arnold 1995). See the Appendix for the mathematical details.

Finally, the CDF or PDF fittings of the adopted distribution functions to the rainfall data are shown in Figs. 13, 14, and 15. These functions were found to have the least KS test values among nominated distribution functions.

Seasonal spells statistics

As discussed earlier, three seasons are proposed for the Jeddah area based on the rain intensity. In this section, an analysis of the seasonal spell durations and their rainfall intensities are presented. Extraction of the spell durations and rainfall intensities is constructed after splitting the rainfall data into the seasons each year. For instance, the first data point slice for the high rain season starts in 1 November 1971 until 31 January 1972. Out of this slice, the dry and wet spell durations are extracted. The process goes on for the next year slice for the same season and the spell durations are concatenated to form a dry spell vector for this season. Similarly, the wet and rainfall intensities of the different seasons are processed. Figure 16 shows the mean values of these quantities for all the stations at the different seasons. It can be clearly noticed that the dry spell durations are shorter in the high rainy seasons and longer in the dry seasons. While the wet spell durations are almost the same for all seasons, the rainfall intensities behave as opposite to the dry spell durations with the different seasons. While the average rainfall intensity in the high rainy season is 9.59 and 6.24 mm/day in the dry season, the average dry spell duration is 24.33 days in the high rainy season and 102.93 days in the dry season. This confirms the earlier conclusion that a more intense rain is expected in shorter period in the high rainy seasons while longer dry days will be in the dry seasons.

Finally, a trend analysis on the seasonal dry and wet spells and rainfall intensities is carried out. Figure 17 shows the trends per year for each station for each season. In high rainy season, the dry spell trends are increasing while the wet spell trends are decreasing and the rainfall intensity trends are increasing for all stations. In low rainy season, the dry spell trends are slightly increasing, while the wet spell trends are decreasing for all stations except for station J134, and rainfall intensity trends are decreasing slightly for most of the stations. In dry season, the dry spell trends are increasing for all stations

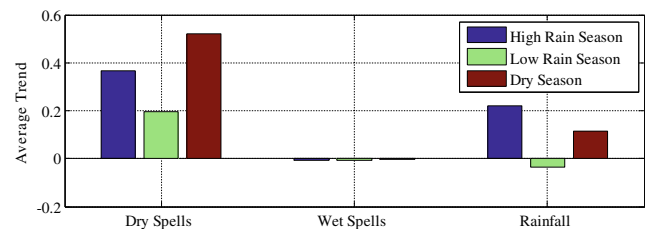


Fig. 18 Average seasonal trends of dry and wet spells and rainfall intensities

except the mountain station (J239), while wet spell trends are decreasing. The rainfall intensity trends, however, are increasing in low altitude stations (J102, J134, and J219), while slightly decreasing for the others. Figure 18 summarizes the average trends across all stations for the three seasons. It shows increase in dry spell in all seasons, where the rainfall intensity trends increase in high rainy season and low rainy in dry season.

Conclusion

Rainfall variability shifts and trends are the most important issues that are influenced by the climate change. The main objectives of the present study are to investigate detailed characteristics of the observed daily rainfall series available in Jeddah area with six stations over the period of 1971–2012 on daily, annual, and seasonal basis. This study shows the detailed features of the dry, wet spells and rainfall intensity. Overall, weak annual repeatability is found in the autocorrelation for every station; however, the cross-correlation between the different stations is noticed for some of the stations while most others have weak responses. In addition, there is no consistency in the storm event occurrences within the different stations.

Monthly rainfall analysis suggested that there are three main rainy seasons, namely high rainy season (November, December, January), low rainy season (February, March, April, October), and dry season (May, June, July, August, September). Furthermore, the study shows that there is a positive trend in the monthly rainfall for the urban stations J102 and J134 in the most risky rainfall storm month of November. In general, the study concluded that the rainy months are getting more intense rainfall while the dry months are getting drier due to the impact of the climate change. The urban station J134 located in Jeddah City is experiencing a positive rainfall trend of 1.09 mm/year/year, which must be taken into consideration for future planning and management.

Autorun analysis is implemented in this study to investigate the properties of the dry, wet durations and rainfall intensities. However, the study shows that the overall average dry spell durations is about 80 continuous days while the average wet spell durations is 1.39 days with an average rainfall

intensity of 8.2 mm/day. Seasonal autorun analysis confirms that the rainy seasons are tending to have more intense rainfall, while the dry seasons are becoming drier. This study concludes that the climate change is affecting the arid region rainfall variability and intensity behavior.

Appendix

Shifted-Geometric distribution

For the Geometric function, the density function is adjusted to:

$$f(x) = p \cdot q^{x-1} \quad x = 1, 2, \dots \tag{4}$$

with a cumulative distribution function as,

$$F(x) = 1 - q^x \quad x = 1, 2, \dots \tag{5}$$

This function is used to generate random numbers from a uniform distribution as follows.

$$F^{-1}(\xi) = \left\lceil \frac{\ln(1-\xi)}{\ln(1-p)} \right\rceil \tag{6}$$

where ξ is a random number generated from a continuous uniform distribution in the range 0 to 1, and p is the Geometric distribution parameter. The $\lceil \cdot \rceil$ function is the integer ceiling value in order to generate random integers. The value of p can be estimated from the data mean value as:

$$p = \frac{1}{\mu} \tag{7}$$

Shifted-Poisson distribution

The original Poisson distribution function is given as follows,

$$f(x) = e^{-\lambda} \frac{\lambda^x}{x!} \quad x = 0, 1, 2, \dots \tag{8}$$

with mean and variance of λ . However, since the wet spells lengths are 1 day or more, the probability mass function needs adjustment. One can simply deduct that the probability $f(x=0)$ and scale the entire mass function to have a unity sum. Thus, the new shifted Poisson-like distribution function becomes as,

$$f_{sp}(x) = e^{-\lambda} \frac{\lambda^x}{x!} \cdot \frac{1}{1-f(0)} \quad x = 1, 2, \dots \tag{9}$$

which yields,

$$f_{sp}(x) = \frac{\lambda^x}{x!} \cdot \frac{e^{-\lambda}}{1-e^{-\lambda}} \quad x = 1, 2, \dots \tag{10}$$

For this distribution, the mean value can be calculated based on the original Poisson mean value as follows.

$$\begin{aligned} \mu &\equiv \sum_{x=1}^{\infty} x \cdot \frac{\lambda^x}{x!} \frac{e^{-\lambda}}{1-e^{-\lambda}} \\ &= \frac{1}{1-e^{-\lambda}} \sum_{x=0}^{\infty} x \cdot e^{-\lambda} \frac{\lambda^x}{x!} \\ &= \frac{1}{1-e^{-\lambda}} \cdot \lambda \end{aligned} \tag{11}$$

Similarly, the cumulative distribution function (CDF) is derived as follows:

$$\begin{aligned} F_{sp}(x) &\equiv \sum_{y=1}^x \frac{\lambda^y}{y!} \frac{e^{-\lambda}}{1-e^{-\lambda}} \\ &= \frac{1}{1-e^{-\lambda}} \left(\sum_{y=0}^x e^{-\lambda} \frac{\lambda^y}{y!} - e^{-\lambda} \frac{\lambda^0}{0!} \right) \\ &= \frac{1}{1-e^{-\lambda}} \left(\frac{\Gamma(x+1, \lambda)}{\Gamma(x+1)} - e^{-\lambda} \right) \\ &= \frac{1}{1-e^{-\lambda}} [F_{\text{pois}}(x_i) - e^{-\lambda}] \end{aligned} \tag{12}$$

where $F^{\text{pois}}(\cdot)$ is the CDF of the original Poisson distribution. Finally, to generate random numbers from the shifted Poisson distribution, uniformly distributed random numbers are first generated in the range [0:1), say ξ_i , are generated and the numbers x_i is solved as follows:

$$\begin{aligned} \xi_i &= F_{sp}(x_i) \\ &= \frac{1}{1-e^{-\lambda}} [F_{\text{pois}}(x_i) - e^{-\lambda}] \end{aligned} \tag{13}$$

from which,

$$\begin{aligned} F_{\text{pois}}(x_i) &= (1-e^{-\lambda}) \cdot \xi_i + e^{-\lambda} \\ x_i &= F_{\text{pois}}^{-1} [(1-e^{-\lambda}) \cdot \xi_i + e^{-\lambda}] \end{aligned} \tag{14}$$

Log Pearson Type III distribution

The Log-Pearson Type III distribution is the best function for the rainfall intensity. Based on the data range, it is given by,

$$f(x) = \begin{cases} \frac{-1}{\beta \Gamma(\alpha) x} \left(\frac{y-\gamma}{\beta} \right)^{\alpha-1} e^{-\frac{y-\gamma}{\beta}} & 0 < x \leq e^\gamma \quad \beta < 0 \\ \frac{1}{\beta \Gamma(\alpha) x} \left(\frac{y-\gamma}{\beta} \right)^{\alpha-1} e^{-\frac{y-\gamma}{\beta}} & x \geq e^\gamma \quad \beta > 0 \end{cases} \tag{15}$$

where $y = \ln(x)$. The moments of the distribution can be estimated for the logarithm of the data, y , rather than the data itself as follows.

$$\begin{aligned}
 \mu_y &= \gamma + \alpha\beta \\
 \sigma_y^2 &= \alpha \beta^2 \\
 E(y - \mu_y) &= 2\alpha\beta^3
 \end{aligned}
 \tag{16}$$

From which the distribution parameters (α , β , and γ) can be estimated in the following order.

$$\begin{aligned}
 \beta &= \frac{\sigma_y}{2} \text{skew}(y) \\
 \alpha &= \frac{\sigma_y^2}{\beta^2} \\
 \gamma &= \mu_y - \alpha\beta
 \end{aligned}
 \tag{17}$$

Open Access This article is distributed under the terms of the Creative Commons Attribution 4.0 International License (<http://creativecommons.org/licenses/by/4.0/>), which permits unrestricted use, distribution, and reproduction in any medium, provided you give appropriate credit to the original author(s) and the source, provide a link to the Creative Commons license, and indicate if changes were made.

References

- Akinremi OO, McGinn SM, Cutforth HW (2001) Seasonal and spatial patterns of rainfall trends on the Canadian prairies*. *J Climate* 14: 2177–2182
- Almazroui M (2011) Sensitivity of a regional climate model on the simulation of high intensity rainfall events over the Arabian Peninsula and around Jeddah (Saudi Arabia). *Theor Appl Climatol* 104:261–276
- Almazroui M, Islam MN, Athar H, Jones PD, Rahman MA (2012) Recent climate change in the Arabian Peninsula: annual rainfall and temperature analysis of Saudi Arabia for 1978–2009. *Int J Climatol* 32:953–966
- Alyamani M, Şen Z (1992) Regional variation of monthly rainfall amounts in the Kingdom of Saudi Arabia. *J King Abdulaziz Univ FES* 6:113–133
- Artlert K, Chaleerakrakoon C, Nguyen VT (2013) Modeling and analysis of rainfall processes in the context of climate change for Mekong, Chi, and Mun River Basins (Thailand). *J Hydro-Env Res* 7:2–17
- Box GE, Jenkins GM, Reinsel GC (1994) *Time series analysis: forecasting and control*, 3rd edn. Prentice-Hall, New Jersey
- Crutzen PJ, Zimmermann PH (1991) The changing photochemistry of the troposphere. *Tellus* 43AB:136–151
- Cryer JD (1986) *Time series analysis*. MA Duxbury Press, Boston
- Davis J (2002) *Statistics and data analysis in geology*, 3rd edn. Wiley, New York
- EasyFit Professional (2009) Version 5.2, <http://www.mathwave.com>
- Feyerherm AM, Bark LD (1965) Statistical methods for persistence precipitation patterns. *J Appl Meteorol* 4:320–328
- Goyal MK (2014) Statistical analysis of long term trends of rainfall during 1901–2002 at Assam, India. *Water Resour Manag* 28:1501–1515
- IPCC (2007) *The physical science basis. Summary for policymakers. Contribution of working group I to the fourth assessment report. The Intergovernmental Panel on Climate Change*. In Solomon S., Qin D, Manning M, Chen Z, Marquis M, Averyt K, Tignor M, Miller H (eds), Cambridge University Press, Cambridge
- Kendall MG (1975) *Rank correlation methods*, 4th edn. Charles Griffin, London, p 202
- Lioubimtseva E (2004) Climate change in arid environments: revisiting the past to understand the future. *Prog Phys Geogr* 28:502–530
- Mann HB (1945) Non-parametric test against trend. *Econometrica* 13: 245–259
- Milton J, Arnold J (1995) *Introduction to probability and statistics: principles and applications for engineering and the computing sciences*, 3rd edn. McGraw Hill, New York
- Ministry of Water and Electricity (2012) *Climate data reports*. Hydrology Division, Riyadh
- Şen Z (1976) Wet and dry periods of annual flow series. *J Hydraul Div* 102:HY10
- Şen Z (1978) Autorun analysis of hydrologic time series. *J Hydrol* 36:75–85
- Şen Z (1983) Hydrology of Saudi Arabia. Symposium on Water Resources in Saudi Arabia. Riyadh, pp A68–A94
- Şen Z (1985) Autorun model for synthetic flow generation. *J Hydrol* 81: 157–170
- Şen Z (2009) Precipitation downscaling in climate modelling using a spatial dependence function. *Int J Glob Warm* 1:1–3
- Subyani AM (2004) Geostatistical study of annual and seasonal mean rainfall patterns in southwest Saudi Arabia. *Hydrol Sci J* 49(5): 803–817
- Subyani AM (2011) Hydrologic behavior and flood probability for selected arid basins in Makkah area, western Saudi Arabia. *Arab J Geosci* 4:817–824
- Subyani AM (2012) Flood vulnerability assessment in arid areas, western Saudi Arabia. *Int J River Basin Manag* 10(2):197–203